SANDIA REPORT

SAND2011-3243
Unlimited Release
Printed May 2011

Isotope Exchange Kinetics in Metal Hydrides I: TPLUG Model

Richard S. Larson, Scott C. James, and Robert H. Nilson

Prepared by
Sandia National Laboratories
Albuquerque, New Mexico 87185 and Livermore, California 94550

Sandia National Laboratories is a multi-program laboratory managed and operated by Sandia Corporation, a wholly owned subsidiary of Lockheed Martin Corporation, for the U.S. Department of Energy's National Nuclear Security Administration under contract DE-AC04-94AL85000.

Approved for public release; further dissemination unlimited.

Issued by Sandia National Laboratories, operated for the United States Department of Energy by Sandia Corporation.

NOTICE: This report was prepared as an account of work sponsored by an agency of the United States Government. Neither the United States Government, nor any agency thereof, nor any of their employees, nor any of their contractors, subcontractors, or their employees, make any warranty, express or implied, or assume any legal liability or responsibility for the accuracy, completeness, or usefulness of any information, apparatus, product, or process disclosed, or represent that its use would not infringe privately owned rights. Reference herein to any specific commercial product, process, or service by trade name, trademark, manufacturer, or otherwise, does not necessarily constitute or imply its endorsement, recommendation, or favoring by the United States Government, any agency thereof, or any of their contractors or subcontractors. The views and opinions expressed herein do not necessarily state or reflect those of the United States Government, any agency thereof, or any of their contractors.

Printed in the United States of America. This report has been reproduced directly from the best available copy.

Available to DOE and DOE contractors from
U.S. Department of Energy
Office of Scientific and Technical Information
P.O. Box 62
Oak Ridge, TN 37831

Telephone: (865) 576-8401
Facsimile: (865) 576-5728
E-Mail: reports@adonis.osti.gov
Online order: http://www.doe.gov/bridge

Available to the public from
U.S. Department of Commerce
National Technical Information Service
5285 Port Royal Rd
Springfield, VA 22161

Telephone: (800) 553-6847
Facsimile: (703) 605-6900
E-Mail: orders@ntis.fedworld.gov
Online order: http://www.ntis.gov/help/ordermethods.asp?loc=7-4-0#online

SAND2011-3243
Unlimited Release
Printed May 2011

Isotope Exchange Kinetics in Metal Hydrides I: TPLUG Model

Richard S. Larson
Hydrogen and Combustion Technology Department

Scott C. James
Robert H. Nilson
Thermal/Fluid Science and Engineering Department

Sandia National Laboratories
P.O. Box 969
Livermore, CA 94551-0969
scjames@sandia.gov

This work was funded by Sandia's Engineering Science Research Foundation under the Physics & Engineering Models discipline.

Abstract

A one-dimensional isobaric reactor model is used to simulate hydrogen isotope exchange processes taking place during flow through a powdered palladium bed. This simple model is designed to serve primarily as a platform for the initial development of detailed chemical mechanisms that can then be refined with the aid of more complex reactor descriptions. The one-dimensional model is based on the Sandia in-house code TPLUG, which solves a transient set of governing equations including an overall mass balance for the gas phase, material balances for all of the gas-phase and surface species, and an ideal gas equation of state. An energy equation can also be solved if thermodynamic properties for all of the species involved are known. The code is coupled with the Chemkin package to facilitate the incorporation of arbitrary multistep reaction mechanisms into the simulations. This capability is used here to test and optimize a basic mechanism describing the surface chemistry at or near the interface between the gas phase and a palladium particle. The mechanism includes reversible dissociative adsorptions of the three gas-phase species on the particle surface as well as atomic migrations between the surface and the bulk. The migration steps are more general than those used previously in that they do not require simultaneous movement of two atoms in opposite directions; this makes possible the creation and destruction of bulk vacancies and thus allows the model to account for variations in the bulk stoichiometry with isotopic composition. The optimization code APPSPACK is used to adjust the mass-action rate constants so as to achieve the best possible fit to a given set of experimental data, subject to a set of rigorous thermodynamic constraints. When data for nearly isothermal and isobaric deuterium-to-hydrogen (D→H) and hydrogen-to-deuterium (H→D) exchanges are fitted simultaneously, results for the former are excellent, while those for the latter show pronounced deviations at long times. These discrepancies can be overcome by postulating the presence of a surface poison such as carbon monoxide, but this explanation is highly speculative. When the method is applied to D→H exchanges intentionally poisoned by known amounts of CO, the fitting results are noticeably degraded from those for the nominally CO-free system but are still tolerable. When TPLUG is used to simulate a blowdown-type experiment, which is characterized by large and rapid changes in both pressure and temperature, discrepancies are even more apparent. Thus, it can be concluded that the best use of TPLUG is not in simulating realistic exchange scenarios, but in extracting preliminary estimates for the kinetic parameters from experiments in which variations in temperature and pressure are intentionally minimized.

Table of Contents

List of Figures

List of Tables

Introduction

It has long been known that hydrogen and its isotopes (e.g., H and D) readily dissolve in certain metals, notably palladium (Pd) [1–3]. Due to small differences in thermochemistry, one isotope is generally stored preferentially over the other [4], thereby making separations possible. Alternatively, storage itself may be the primary goal, with one isotope being used to flush out the other when needed. Measured and controlled hydrogen isotope exchange with Pd is in fact routinely carried out, but the physical and chemical aspects of this process are not yet fully understood.

Palladium hydride can exist in two distinct phases, α and β. However, the former is capable of storing only small amounts of hydrogen (up to perhaps $PdH_{0.02}$ around room temperature) and is of no interest here. At room temperature and pressures near atmospheric, only the β phase can exist, with a stoichiometry of roughly $PdH_{0.7}$. The equilibrium hydrogen content decreases modestly with temperature and increases slowly with pressure. It is of course this phase that is used in storage applications. Quantitative equilibrium data in the form of pressure-concentration-temperature plots are available [5,6].

The dissolution of hydrogen isotopes in both the α [7–9] and β [10–12] phases has been studied to determine diffusion rates for H and D in the solid. However, for most systems of interest, exchange rates are limited not by diffusion but by surface reactions; only for large Pd particles at low temperatures does the former limit the exchange [13–15]. Many researchers have examined specific aspects of the exchange process [16–23], and still others have proposed mathematical models [24–29], but significant uncertainties remain with regard to the physics and chemistry that must be included to yield a predictive model.

The work presented here is part of a larger effort to develop a comprehensive modeling capability for hydrogen and deuterium exchange over a powdered Pd bed. The final model is expected to involve significant complexities in both transport and chemistry, but including all of these from the beginning is probably not feasible. Thus, the goal here is to use a simple but roughly adequate transport model as a platform for the development, testing, and optimization of a reasonably detailed multistep surface reaction mechanism. The latter can then be used as a starting point for the mechanism ultimately chosen for incorporation into a more sophisticated transport model. As usual, unknown kinetic parameters in the current study are inferred by matching simulation results for time-dependent effluent concentrations to suitable experimental data. Obviously, this procedure is most likely to give reasonable results if the experimental conditions do not seriously violate the assumptions underlying the reactor model. We have therefore chosen to focus on the slow and nearly isothermal exchanges carried out by Foltz and Melius (F&M) [30–32]. They studied both D→H (slightly exothermic replacement of dissolved D with H) and H→D (slightly endothermic replacement of dissolved H with D), and both processes are simulated here with the same reaction mechanism (all steps being reversible). A similar procedure is then carried out for the experiments of Outka and Foltz (O&F) [33], which have an additional complicating factor in the form of a surface poison (CO). Finally, an attempt is made to fit the data from a blowdown experiment, which is characterized by rapid changes in temperature and pressure. This is not expected to produce reliable values for the kinetic parameters, but the degree to which they differ from those extracted from the F&M experiments may provide an indication of the adequacy (or lack thereof) of the simple transport model in this situation.

The reactor model used in the simulations here is the Sandia in-house code TPLUG, with suitable modifications being made to the input files to allow application to a powder bed rather than the traditional empty tube. The code uses Chemkin [34] to handle the specified surface reaction mechanism (gas-phase reactions being assumed to be irrelevant). The optimization of the unknown parameters (rate constants and surface site densities) in the Chemkin input file is carried out by the APPSPACK [35] software package. Specifically, the parameters are varied, subject to rigorous thermodynamic constraints, so as to minimize the root-mean-square deviation between the experimental effluent gas concentrations and those obtained from the TPLUG simulations.

The TPLUG Model

A description of the reactor model embedded within TPLUG and the surface reaction mechanism chosen for this study is given here.

Reacting Flow Equations

In TPLUG, the transient governing equations for a plug flow reactor are discretized in the spatial (axial) direction, and the resulting set of ordinary differential equations is integrated in time with the DASAC [36] software. The set of governing equations comprises an overall continuity equation for the gas, material balances for all of the gas-phase and surface species, and an ideal gas equation of state. An energy equation is also available, but it is not needed to simulate the F&M and O&F experiments, because the slow exchange processes were nearly isothermal. Furthermore, while the experiments involved axial pressure gradients of roughly 20 Torr/cm, these have been found to have little or no effect on the simulation results, so they are neglected as well.

For a plug flow reactor, the gas-phase continuity equation is

$$A_c \frac{\partial \rho}{\partial t} = -\frac{\partial}{\partial x}\left(\rho u A_c\right) + a_i \sum_{\text{gas}} s_k M_k , \tag{1}$$

where t (s) and x (cm) are the time and spatial variables, ρ (g/cm^3) is the mass density of the gas, u (cm/s) is the axial velocity, A_c (cm^2) is the cross-sectional area of the channel, a_i (cm) is the surface area per unit length, M_k (g/mol) is the molecular weight of species k, and s_k (mol/cm^{2}s) is the molar production rate of this species per unit area. The corresponding material balance for gas-phase species k is

$$A_c \rho \left(\frac{\partial Y_k}{\partial t} + u \frac{\partial Y_k}{\partial x} \right) = M_k \left(s_k a_i + g_k A_c \right) - a_i Y_k \sum_{\text{gas}} s_j M_j , \tag{2}$$

where Y_k (−) is the mass fraction of this species and g_k (mol/cm^{3}s) is its molar production rate per unit volume by homogeneous gas reactions. By assumption, all reactions involved in D→H and H→D exchanges take place in or on the solid, so g_k is set to zero. Assuming further that there is no axial transport of the surface species in the reactor (i.e., that D/H atoms do not move from particle to particle), the material balance for each of them takes the simple form

$$\frac{\Gamma}{\sigma_k}\frac{\partial x_k}{\partial t} = s_k, \tag{3}$$

where Γ (mol/cm^2) is the site density of the surface phase in question (based on the actual surface area), x_k (−) is the site fraction of species k in this phase, and σ_k (−) is the site occupancy number (i.e., the number of sites covered per admolecule) for this species. Finally, the gas-phase equation of state is simply

$$PM = \rho RT, \tag{4}$$

where P (dyne/cm^2) is the pressure, M (with no subscript; g/mol) is the average molecular weight of the mixture, R (erg/mol·K) is the universal gas constant, and T (K) is the absolute temperature.

Because TPLUG is nominally meant to describe reacting flow in an open tube, with surface reactions taking place only on the wall, its application to packed-bed reactors is not completely straightforward. First, it is necessary to correct the actual tube diameter for the porosity of the bed to obtain the cross-sectional area available for flow. In addition, the surface area available for reaction is calculated from the stated specific surface-to-volume ratio of the bed particles. It should be emphasized that, for purposes of simulation with Chemkin, all of the solid phase species involved are treated as surface species, and all of the reactions taking place are treated as surface reactions, notwithstanding the use of the term bulk in some cases. Because of this, all concentrations of non-gaseous species are per unit area, each being equal to the product of a site fraction and the site density of the surface phase upon which the species resides.

Isotope Exchange Chemistry

Isotope exchange mediated by a solid (surface and/or bulk) can be described at various levels of detail. In their modeling work, F&M used a simple mechanism consisting of the two gas-solid reactions in the left-hand panel of Figure 1. Thus, they did not attempt to distinguish surface and bulk H (or D) atoms, arguing that bulk diffusion was much faster than the surface exchanges, which was likely true during their slow exchange experiments. Regardless of the rate-limiting mechanism, it is clear that each exchange is unlikely to proceed in a single concerted step, as pictured, so this should be regarded as a global description of the chemistry. A plausible description in terms of more elementary reactions, as proposed by O&F [33], is shown in the right panel. Here each gas-phase diatomic molecule must dissociate on the surface, and each adsorbed atom can either move into the bulk of the solid or combine with another surface atom and desorb. However, the picture implies (and O&F assumed for simplicity) that movement into the bulk is *necessarily* accompanied by movement of another atom in the opposite direction. In general this is not true, so a net creation or disappearance of vacancies in the bulk (as well as on the surface) is possible. An enhanced version of the O&F scheme that incorporates this phenomenon will be the basis of the modeling work described here.

Thus, the chemical mechanism chosen to represent both the D→H and H→D exchange processes involves the three familiar gas-phase species (H_2, HD, and D_2) as well as six solid-phase species: H_s, D_s, V_s, H_b, D_b, and V_b. To reiterate, subscript "s" denotes a species that actually resides on the particle surface and is thus in contact with the gas, while "b" denotes a species residing in one of the bulk layers below (all of which are lumped together). In this scheme there is no direct communication between the gas and the bulk. The symbol V denotes a vacant site, in keeping with the fact that the available storage sites in the metal are never fully occupied.

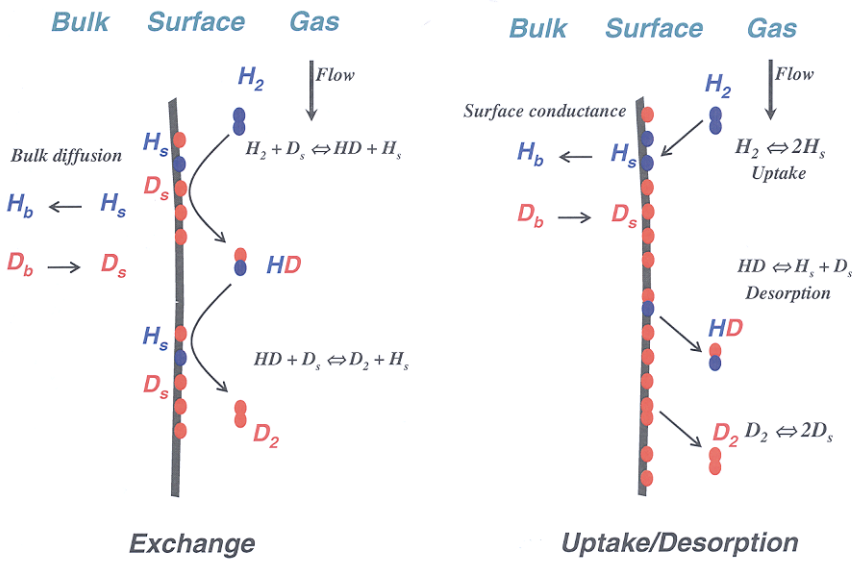

Figure 1. Two conceptual models for hydrogen isotope exchange.

Drawing from Figure 1, the following set of reactions (which allows for possible surface poisoning by CO) is the simplest way to represent the exchange processes in terms of elementary reactions while still acknowledging the independent role of the surface and the potential for creation of bulk vacancies:

$$H_2 + 2V_s \Leftrightarrow 2H_s \quad \text{(R1)}$$

$$HD + 2V_s \Leftrightarrow H_s + D_s \quad \text{(R2)}$$

$$D_2 + 2V_s \Leftrightarrow 2D_s \quad \text{(R3)}$$

$$CO + V_s \Leftrightarrow CO_s \quad \text{(R4)}$$

$$H_s + V_b \Leftrightarrow H_b + V_s \quad \text{(R5)}$$

$$D_s + V_b \Leftrightarrow D_b + V_s \quad \text{(R6)}$$

The forward and reverse rate constants for reaction (R*i*) are k_i and k_{-i}, respectively. Clearly, the reactions must be reversible if the mechanism is to be capable of describing exchange in either direction. Note that there is no *direct* exchange between H and D; while such a reaction could be obtained by subtracting (R6) from (R5),

$$H_s + D_b \Leftrightarrow H_b + D_s$$

this would be less general than the path chosen and would probably not be elementary.

We set aside for the moment the poisoning reaction (R4). Then, because the reactions are reversible and because two Arrhenius parameters (a pre-exponential factor and an activation energy) are necessary to specify the rate constant in each direction, it would appear that 20 parameters are needed. These are in addition to the site densities for the two surface phases, which are also treated as unknown. However, when simulating the F&M and O&F experiments, several factors reduce the number of necessary parameters. First, because the simulations are isothermal, the activation energies are irrelevant and may be chosen arbitrarily, with the understanding that the results are *not* applicable at any other temperature; this reduces the number of unknown kinetic parameters to 10. (If another data set were available for exchanges at a different temperature, then the activation energies could also be estimated by fitting both data sets simultaneously.) A further reduction is possible through imposition of thermodynamic constraints on the mechanism. Because there are only two nontrivial species with unknown thermodynamic properties, namely H_s and D_s, only two equilibrium constants can be specified arbitrarily (i.e., for only two reactions can the forward and reverse rate constants be varied freely). We choose these reactions to be the dissociative adsorptions (R1) and (R3). For the remaining reactions, the rate constants in the two directions must be related in such a way as to be consistent with known thermochemistry, as will now be shown.

Note first that forming the linear combination (R1) + 2 × (R5) gives

$$H_2 + 2V_b \Leftrightarrow 2H_b, \tag{R7}$$

which describes the overall dissolution of H_2 in Pd, the thermochemistry of which has been studied extensively. It follows that the equilibrium constants for the reactions are related by

$$K_7 = K_1 K_5^2, \tag{5}$$

and therefore

$$k_{-5} = k_5 \left(\frac{k_1}{k_{-1} K_7} \right)^{1/2}. \tag{6}$$

The equations for the D isotope are analogous, using the combination (R3) + 2 × (R6):

$$D_2 + 2V_b \Leftrightarrow 2D_b \tag{R8}$$

$$K_8 = K_3 K_6^2 \tag{7}$$

$$k_{-6} = k_6 \left(\frac{k_3}{k_{-3} K_8} \right)^{1/2} \tag{8}$$

Finally, forming the combination (R1) + (R3) – 2 × (R2) gives

$$H_2 + D_2 \Leftrightarrow 2HD, \tag{R9}$$

which is the well-known gas-phase equilibration. Thus

$$K_9 = \frac{K_1 K_3}{K_2^2} \tag{9}$$

and

$$k_{-2} = k_2\left(\frac{k_{-1}k_{-3}K_9}{k_1k_3}\right)^{1/2}. \tag{10}$$

The implication of these equations is that, in the data fitting process, only for (R1) and (R3) can the rate constants be specified arbitrarily in both directions if thermodynamic consistency is to be maintained. Because K_7, K_8, and K_9 can be obtained from the literature, the reverse rate constants for (R2), (R5), and (R6) are fixed by Eqs. (10), (6), and (8), respectively, once the forward rate constants are chosen. This reduces the number of adjustable kinetic parameters to seven. More generally, if all quantities are expressed in Arrhenius form, then the equations provide constraints on both the pre-exponential factors and the activation energies.

The equilibrium constant K_9 is well known [30]:

$$K_9 = 4.242\exp\left(-\frac{0.649}{RT}\right), \tag{11}$$

where RT is in kJ/mol. (Note that Chemkin allows the use of non-cgs units for energy terms like this.) The thermochemistry of the dissolution reactions has been studied by Santandrea and Behrens [37], as quoted by Charton et al. [29]. After some manipulation, their results can be expressed as

$$K_7 = 2.050\times10^{-4}T\exp\left(\frac{100.35 - 90.04x_{\mathrm{H}}}{RT}\right) \tag{12}$$

and

$$K_8 = 2.265\times10^{-4}T\exp\left(\frac{95.53 - 90.04x_{\mathrm{D}}}{RT}\right), \tag{13}$$

where T is in Kelvins, K_7 and K_8 are in cm^3/mol, and x represents the solid-phase stoichiometry, i.e., the number of dissolved H or D atoms per Pd atom, which is equivalent to the site fraction used by Chemkin. The presence of the site fractions in these equations implies that the heats of solution are composition-dependent, which is a type of nonideal behavior. Equations (6) and (8) then show that k_{-5} and k_{-6} must have composition-dependent activation energies. Fortunately, Chemkin has the flexibility to handle this situation, but there is an additional complication. Equations (12) and (13) refer to situations in which only a single component (H_2 or D_2) is present in the gas, so they are not completely general. When both H and D are present, it is logical to expect that both K_7 and K_8 will depend on both x_{H} and x_{D}. If the two isotopes were energetically equivalent, then the sum $x_{\mathrm{H}} + x_{\mathrm{D}}$ could be used in both equations, but a still more general approach is to write

$$K_7 = 2.050\times10^{-4}T\exp\left(\frac{100.35 - 90.04x_{\mathrm{H}} - 2\beta x_{\mathrm{D}}}{RT}\right) \tag{14}$$

and

$$K_8 = 2.265\times10^{-4}T\exp\left(\frac{95.53 - 2\beta x_{\mathrm{H}} - 90.04x_{\mathrm{D}}}{RT}\right). \tag{15}$$

The use of the same value of β in these two equations is essential for consistency with the Gibbs-Duhem equation. Because β is unknown, it is treated as another adjustable parameter. Together with the seven kinetic constants and the two site densities, this gives a total of ten parameters to be estimated by fitting the effluent concentration data.

A complete derivation of Eqs. (14) and (15) from the equilibrium relations of Santandrea and Behrens [37] is presented in Appendices A and B. Appendix B also gives a detailed discussion of the methods that can be used to compute the species thermodynamic properties that are needed for non-isothermal simulations. Finally, Appendix C shows how the coupling between adjustable parameters can be weakened in order to improve the efficiency of the optimization process.

Application to the Foltz & Melius Experiments

In this section we summarize an attempt to fit the data from the slow and nearly isothermal exchange experiments of Foltz and Melius [30] with the TPLUG model, using the reaction mechanism consisting of (R1)–(R6) (neglecting (R4) initially, but including it later). The modeling work carried out by F&M is not a primary concern here, but some aspects of it are discussed below and in Appendix D.

As noted earlier, because TPLUG is nominally designed to simulate reacting flow in an open tube with surface reactions taking place on the wall, its application to a packed-bed reactor requires some parameter modifications. For the F&M experiments, the effective tube diameter is 0.5568 cm to yield the cross-sectional flow area corrected for porosity (0.31). The surface area per unit length is computed to be 275 cm, based on the stated value of 507.6 cm^{-1} for the specific surface-to-volume ratio of the bed particles and the *actual* cross-sectional area of 0.7854 cm^2. Finally, the equilibrium relations (A.1) and (A.2) are used to obtain the initial compositions of the hydrided and deuterided beds; these are x_H = 0.7127 and x_D = 0.6730, corresponding to average pressures of 1.234 atm and 1.270 atm, respectively, and a temperature of 300 K. Whether these pressures are truly the best to use is not important, because the equilibrium compositions are fairly insensitive to them. For example, lowering the H_2 pressure to 1 atm causes the value of x_H to fall only to 0.7081.

Because the chemical mechanism is meant to describe both the D→H and H→D exchange processes, a single set of parameters is used to fit both data sets simultaneously. The resulting site densities are 2.938×10^{-7} mol/cm^2 and 1.959×10^{-4} mol/cm^2 for the surface and bulk phases, respectively. The wide disparity in these values is expected, because the vast majority of the Pd atoms must reside below the actual surface in the 115 μm-diameter particles of these experiments. Reassuringly, the bulk density is fairly close to the theoretical value of 2.23×10^{-4} mol/cm^2. The mass-action rate constants at 300 K are listed in Table 1. As a check, the value of K_1K_3/K_2^2 corresponding to these values is 3.273, which is consistent with (11). Comparison of k_5 with k_6 and k_{-5} with k_{-6} shows that the migration of H atoms between the surface and the bulk is much faster than the corresponding process involving D. Unfortunately, this appears to conflict with the diffusivity data quoted by Hamilton [15].

A comparison of the simulated effluent curves with the experimental data for both the D→H (deuterium-loaded bed flushed with hydrogen) and H→D (hydrogen-loaded bed flushed with deuterium) exchanges is shown in Figure 2.

Table 1. Estimated rate constants from fitting of F&M data with no CO poisoning.

Parameter	Estimated value
k_1 (cm^5/mol^{2}s)	1.155×10^{18}
k_{-1} (cm^2/mol·s)	2.290×10^{7}
k_2 (cm^5/mol^{2}s)	4.390×10^{17}
k_{-2} (cm^2/mol·s)	1.263×10^{7}
k_3 (cm^5/mol^{2}s)	4.385×10^{17}
k_{-3} (cm^2/mol·s)	5.593×10^{6}
k_5 (cm^2/mol·s)	4.505×10^{6}
k_{-5} (cm^2/mol·s)	$7.482\times10^{3}\ \exp(18.05x_H + 17.79x_D)$
k_6 (cm^2/mol·s)	2.895×10^{5}
k_{-6} (cm^2/mol·s)	$1.499\times10^{3}\ \exp(17.79x_H + 18.05x_D)$

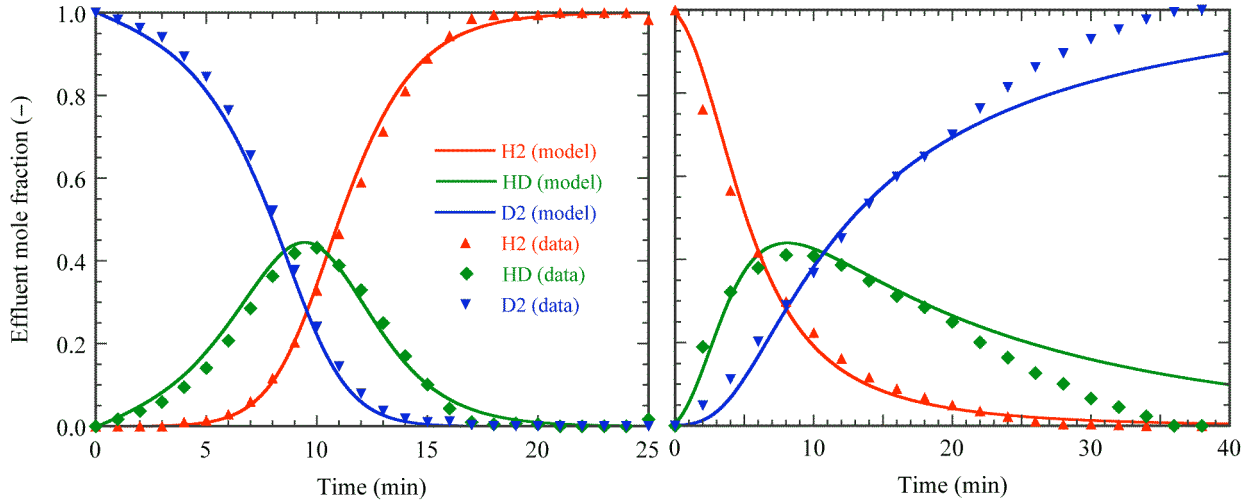

Figure 2. Exit gas compositions for the D→H (left) and H→D (right) exchanges from the F&M experiments (symbols) and best-fit TPLUG simulations (curves).

Clearly, the fit in Figure 2 for the D→H exchange is fairly good, while the H→D simulation is lacking at late times. A variety of attempts to solve this problem, such as introducing multiple bulk layers, have not proven to be any more successful. Similar behavior was reported by F&M, although their H→D simulation begins to deviate from the data at an even earlier time. (Actually, F&M *fitted* only the D→H data and then *predicted* the H→D curves, so their simulation for D→H is very good while that for H→D is quite poor.) Given the large number of adjustable parameters in the current study, a better fit for H→D could have been expected. The mediocre result suggests that (a) the details of the chemical mechanism are not very important, as stated by F&M [30]; and (b) the F&M and TPLUG-based models probably have a common flaw that prevents the long-time H→D behavior from being captured correctly, i.e., some aspect of the physics of exchange is not modeled adequately. One possibility is internal diffusion within the particles, although recent work by Hamilton [15] suggests that this is not a likely candidate.

Among the processes that could, in theory, affect the results is blocking of surface sites by a foreign substance adsorbed from the gas stream. In fact, the H→D simulation can be improved dramatically if such a poison is assumed to be present, although this is purely speculative. From the stated purities of the H_2 and D_2 feed streams (99.9995% and 99.99% [30]), one can hypothesize contaminant levels of 5 ppm and 100 ppm, respectively. By assigning these levels to CO, adding reaction (R4) to the chemical mechanism, and refitting the data, it is possible to obtain excellent results. Remarkably, even better results can be achieved with a contaminant level of just 5 ppm in *both* streams; these new fits are shown in Figure 3. It must be mentioned that the simulations with poisoning predict that the isotope exchanges within the bed are not complete (i.e., some of the original isotope is never flushed out), especially for H→D. We are aware of no direct evidence to support this, although the amount of H liberated during the H→D experiment is indeed about 7% less than the amount of D released by D→H.

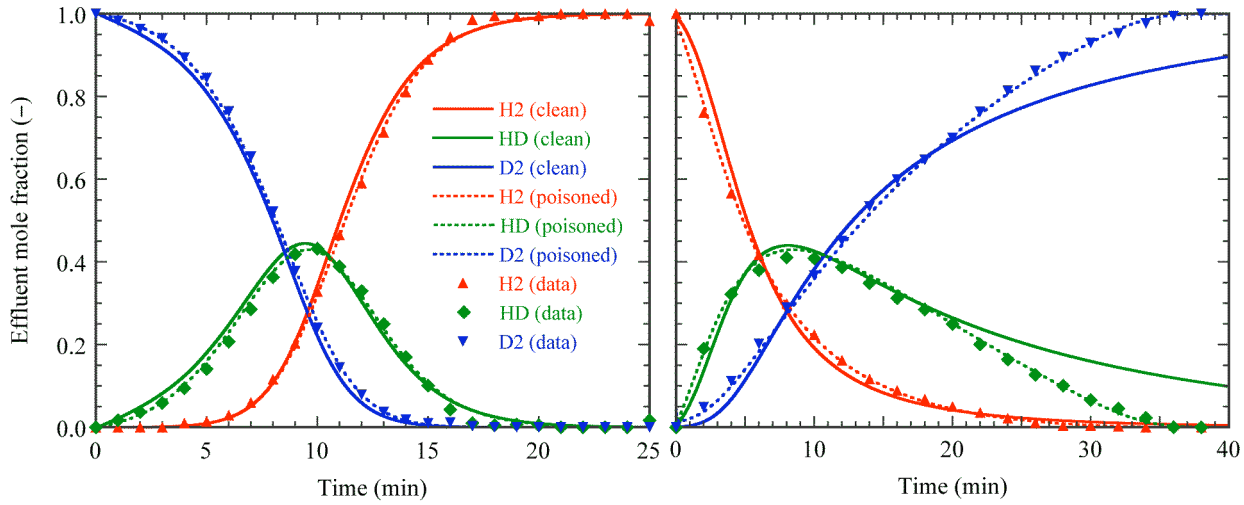

Figure 3. TPLUG fits (curves) to the F&M experiments (symbols) assuming both pure and CO-poisoned feed streams.

Finally, an interesting aspect of both the F&M model and the experimental data should be mentioned. In the presentation of the model, it is stated explicitly that the three gas-phase species are assumed to be at equilibrium at all times and at all points in the bed. However, Figure 4 shows that the experimental effluent concentrations are not at all consistent with this. Because the F&M model conflicts, in this sense, with the data that it is trying to fit, the validity of their simulation results is questionable, despite their relative success using only two adjustable parameters. It is interesting to note that the values in Figure 4 tend to cluster around a value of slightly less than 2.0, because a value of $(3.270)^{1/2} = 1.808$ would be the correct theoretical value if reaction (R9) were halved, i.e., if it were written for a single molecule of HD. It should also be noted that the HD pressures in the F&M experiments were apparently not measured directly, but were instead computed from the measured H_2 and D_2 pressures. However, because the HD pressures were computed by *difference* (using the total pressure) rather than from an equilibrium assumption, and because there is considerable scatter in Figure 4, it appears that the clustering is not due to the use of an erroneous value for K_9.

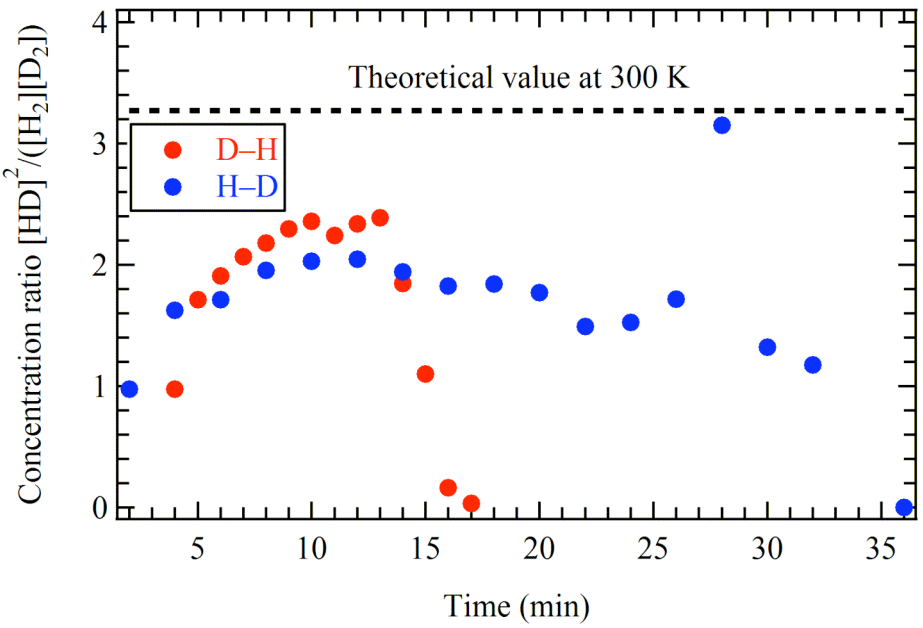

Figure 4. Apparent equilibrium constant for $H_2 + D_2 = 2HD$ in the F&M experiments.

Application to the Outka & Foltz Experiments

Outka and Foltz [33] performed experiments similar to those of Foltz and Melius [30], using ostensibly the same bed material. Unfortunately (for our purposes), they carried out only D→H exchanges, but they investigated explicitly the role of surface poisons by adding various levels of CO (0, 10, 40, and 1800 ppm) to the H_2 feed stream. These data allow a further test of the TPLUG model and the mechanism consisting of (R1)–(R6). However, it should be noted that the H_2 and HD concentrations reported by O&F for the "clean" (0 ppm) experiment are quite different from those of F&M, even though the experimental conditions were almost identical. Therefore, the fitting procedure cannot be expected to produce the same values for the site densities and kinetic parameters as before.

In the TPLUG simulations, the temperature and pressure are set to 298.15 K and 1.320 atm, respectively, the latter being the average value in the bed. The initial deuterium loading of the bed is then $x_D = 0.6758$. All four of the experimental data sets are fitted simultaneously to extract estimates for the site densities and kinetic parameters.

The actual fits to the data are shown in Figure 5. Clearly, high levels of poisoning inhibit trapping of the flush gas and cause the exchange to be incomplete. The model is reasonably successful in accounting for the effect of the CO concentration on the effluent gas traces, as was the model proposed by O&F. The current model actually does a better job in reproducing the long-time behavior at modest levels of poisoning, but it tends to be lacking at short times. Furthermore, it chronically underpredicts the peak level of HD during the exchange. O&F argued that surface poisoning could account for the failure of HD to achieve a level corresponding to equilibrium with H_2 and D_2, although (as noted above) this actually occurs even with a presumably clean bed. The experimental data obviously show this trend, and the site-blocking mechanism can account for it, but the present model overestimates the effect.

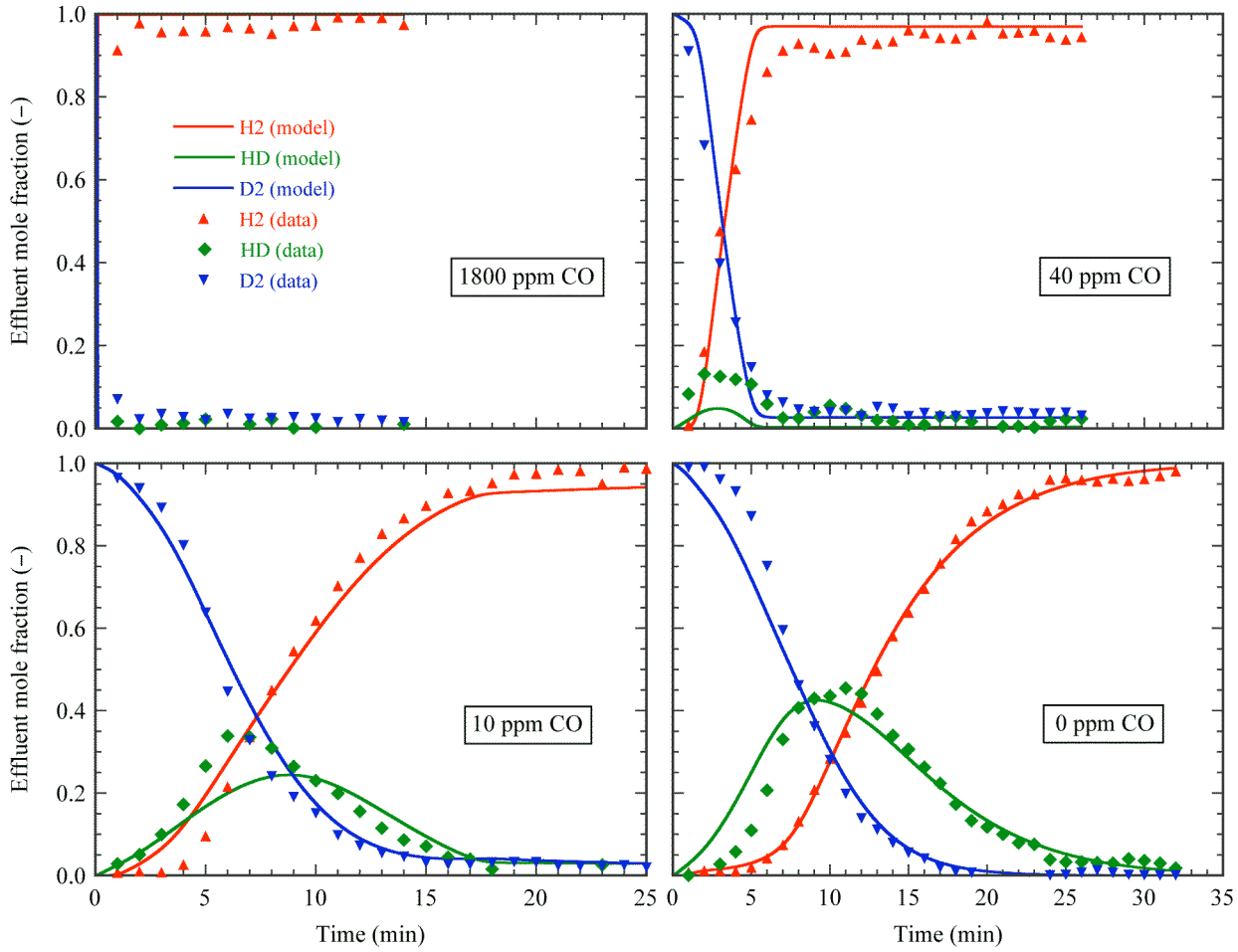

Figure 5. TPLUG fits (curves) to O&F data (symbols) for D→H exchange in the presence of various levels of CO in the feed stream.

The surface and bulk site densities obtained from the data fitting are 1.467×10^{-9} mol/cm^2 and 2.021×10^{-4} mol/cm^2, respectively. The latter is close to the value inferred from the F&M experiments, suggesting that this number is fairly trustworthy. This accords with the fact that the bulk site density is essentially the storage capacity of the bed, whose apparent value should be determined by the gross exchange behavior and be unaffected by the underlying details. On the other hand, the surface site density obtained here is more than two orders of magnitude smaller than the value obtained earlier. However, this discrepancy is not nearly as serious as it appears. If the F&M simulation is repeated using the new site density, with all rate constants scaled to compensate, then the objective function used to measure the quality-of-fit is degraded by an almost trivial 0.7%. By contrast, if the O&F simulation is similarly repeated with the old site density, the objective function is increased by 493%. This strongly suggests that the new site density is the more reliable, and this is consistent with the contention of O&F that poisoning experiments are necessary to elucidate the true role of the surface.

The rate constants inferred from the fitting process are listed in Table 2. At first glance these appear to differ greatly from the corresponding values in Table 1. However, much of the difference can be attributed to the reduction in the surface site density just discussed. For example, because reaction (R1) is second-order in the surface species V_s, reducing the site density by a factor of 200 might be expected to increase k_1 by a factor of 40,000. It can be seen that this effect does in fact account for most of the change. Furthermore, the *equilibrium* constants (i.e., the rate constant ratios) for the various reactions are not drastically different between the two sets. Still, there are some changes in the magnitudes and the trends that cannot be explained so easily. These probably result from two distinct issues: (1) There are insufficient data to allow such a large number of parameters to be determined with confidence; and (2) As noted above, there are genuine differences between the F&M and O&F data sets, making differences in the extracted parameters inevitable.

Table 2. Estimated rate constants from fitting of O&F data.

Parameter	Estimated value
k_1 (cm^5/mol^2s)	5.065×10^{23}
k_{-1} ($cm^2/mol\cdot s$)	5.285×10^{12}
k_2 (cm^5/mol^2s)	2.622×10^{22}
k_{-2} ($cm^2/mol\cdot s$)	1.783×10^{11}
k_3 (cm^5/mol^2s)	4.827×10^{22}
k_{-3} ($cm^2/mol\cdot s$)	6.550×10^{10}
k_4 ($cm^3/mol\cdot s$)	5.646×10^{11}
k_{-4} (s^{-1})	1.177×10^{-2}
k_5 ($cm^2/mol\cdot s$)	5.897×10^{9}
k_{-5} ($cm^2/mol\cdot s$)	$1.195\times10^{7}\ \exp(18.16x_H + 17.24x_D)$
k_6 ($cm^2/mol\cdot s$)	4.977×10^{9}
k_{-6} ($cm^2/mol\cdot s$)	$7.037\times10^{7}\ \exp(17.24x_H + 18.16x_D)$

Application to a Blowdown Experiment

As a final test of the TPLUG model, we attempt to simulate the fast (< 5 s) exchange that occurs during a D→H blowdown experiment in a shorter reactor and with a different Pd powder, using the same (CO-free) chemical mechanism. The chances of success for this effort are dubious, because TPLUG was not designed to handle the rapid and complicated pressure variations that occur during an event of this type. Moreover, data from the experiment show a temperature rise of about 60°C, which could certainly affect the rate constants. Nevertheless, the simulation is carried out using a constant temperature of 300 K and a constant pressure of 2.64 atm, giving an initial x_D of 0.6892. The effective channel diameter is 3.08 cm, corresponding to a porosity of 0.75, and the surface area per unit length is 82,090 cm. The large surface area is due to bed particles that are far smaller than those used in the F&M experiments (1 μm vs. 115 μm).

The site densities extracted from the fitting process are 3.432×10^{-8} mol/cm^2 and 4.160×10^{-6} mol/cm^2 for the surface and bulk phases, respectively. The bulk site density is much

smaller than the value inferred from the F&M fitting, undoubtedly due to the much larger surface area. In fact, if this density is multiplied by the surface area per unit volume and then corrected for porosity (thus giving the number of sites per unit solid volume), the result is actually greater than the corresponding value for F&M, but only by a factor of 1.4. Considering the questionable validity of the model, this is fairly good agreement, although (as noted earlier) the storage capacity of the bed should be one of the easier parameters to estimate accurately.

The mass-action rate constants for the reactions in the mechanism are listed in Table 3. Obviously, there are significant differences between these results and the corresponding values from the F&M fitting. Again, some, but by no means all, of the discrepancies can be ascribed to the changes in the site densities. Of particular note is the fact that deuterium exchange between the surface and the bulk is now predicted to be much faster than that of hydrogen. This conflicts with Table 1 but is actually more consistent with the diffusivities quoted by Hamilton [15]. In truth, if (as is likely) transport between the surface and the bulk is not a rate-limiting step, then the corresponding coefficients inferred from overall exchange data must be considered highly unreliable. Therefore, it is probably not worthwhile to ascribe a great deal of significance to their values, even in a relative sense.

Table 3. Estimated rate constants from fitting of blowdown data.

Parameter	Estimated value
k_1 (cm^5/mol^2s)	3.373×10^{19}
k_{-1} ($cm^2/mol\cdot s$)	3.411×10^{11}
k_2 (cm^5/mol^2s)	2.315×10^{19}
k_{-2} ($cm^2/mol\cdot s$)	2.552×10^{11}
k_3 (cm^5/mol^2s)	3.267×10^{19}
k_{-3} ($cm^2/mol\cdot s$)	1.200×10^{11}
k_5 ($cm^2/mol\cdot s$)	3.892×10^{10}
k_{-5} ($cm^2/mol\cdot s$)	$2.862\times10^{6}\ \exp(18.05x_H + 18.22x_D)$
k_6 ($cm^2/mol\cdot s$)	3.879×10^{11}
k_{-6} ($cm^2/mol\cdot s$)	$1.184\times10^{8}\ \exp(18.22x_H + 18.05x_D)$

The best fit to the experimental data is shown in Figure 6. The quality of the fit is not particularly good, given that even a crude model can reproduce the timing of the HD peak and the H_2-D_2 crossover. While the simulated HD curve is somewhat asymmetric, it is much less so than are the data. More importantly, the predicted peak concentration of HD is too high by a factor of about 2, although it is still slightly smaller than the value corresponding to equilibrium with H_2 and D_2. In fact, modeling results aside, Figure 7 shows that the experimental concentrations of HD are much smaller than those that would be expected at equilibrium. It would seem to be worthwhile to investigate why the intermediate HD is chronically under-produced, even in experiments with clean powder beds. Clearly, the direct measurement of the HD concentration, along with those of H_2 and D_2, would eliminate a principal source of uncertainty.

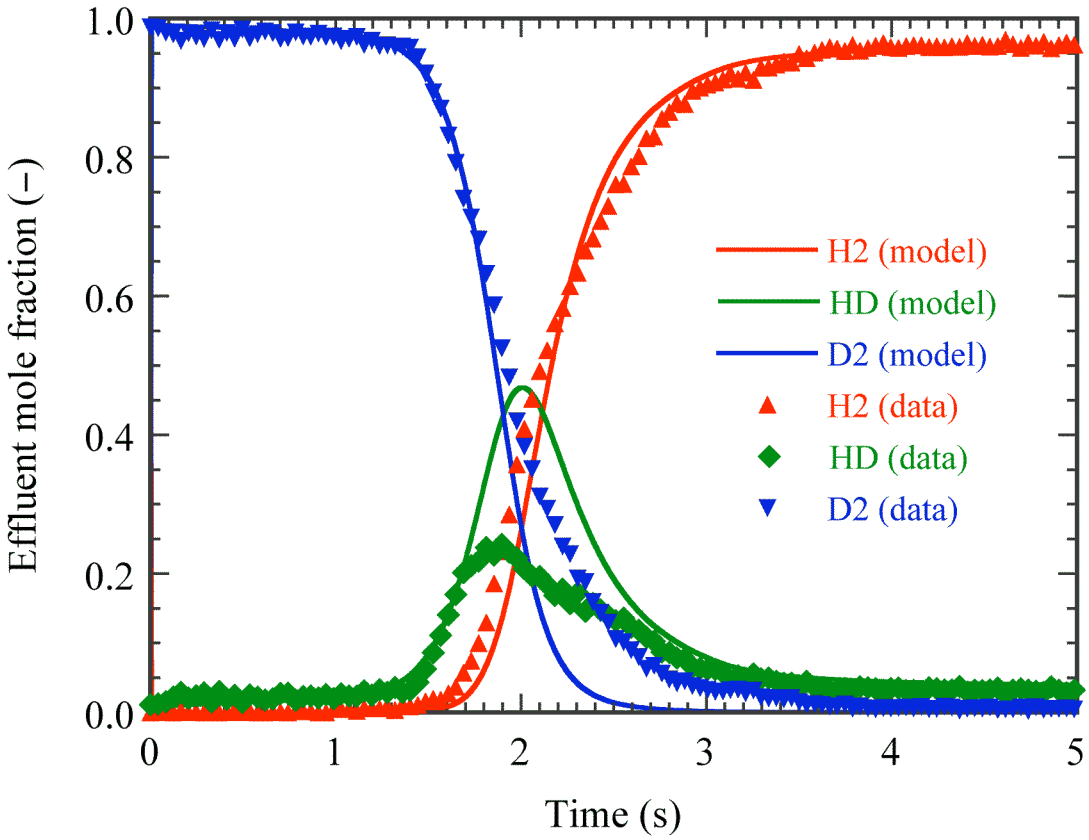

Figure 6. Exit gas composition for the blowdown D→H exchange.

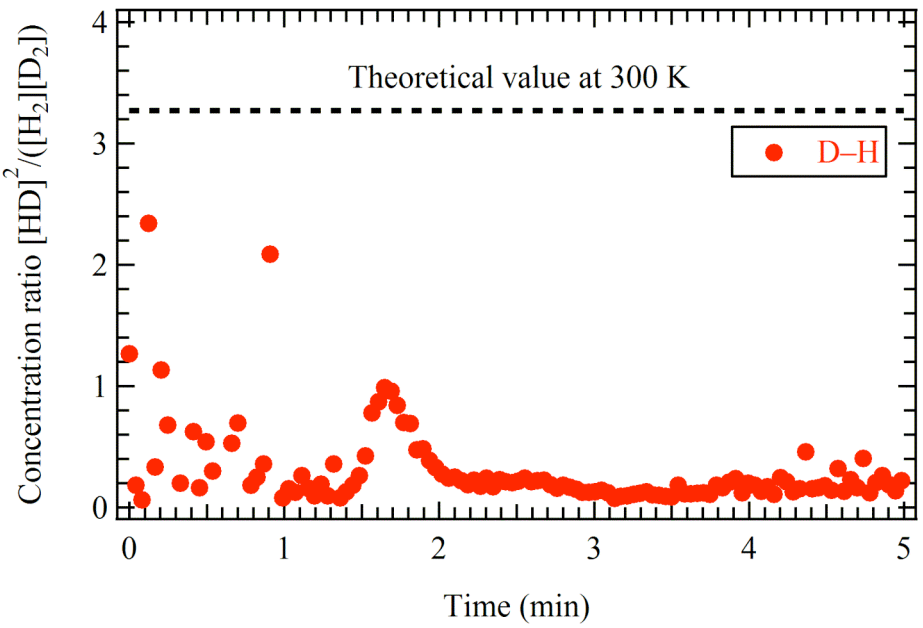

Figure 7. Apparent equilibrium constant for the experimental data of Figure 6.

Conclusions

Overall, the combination of the TPLUG reactor model and the six-step elementary reaction mechanism is reasonably successful in reproducing experimental data for D→H and H→D exchanges in a Pd bed. However, simply matching the basic features of the effluent curves, such as the time of peak HD production, is not a challenging task. If the model is to represent an advance by itself, it should be able to account for finer details, such as the long-time behavior seen in the F&M data for the H→D exchange. However, we have shown that the reaction mechanism used here, even with its many adjustable parameters, is incapable of explaining this particular detail unless the possibility of poisoning in a supposedly clean system is invoked. If poisoning is not the answer, then the explanation apparently lies in some transport mechanism that is missing from both TPLUG and the model used by F&M. In that case, the value of the TPLUG simulations is simply in providing a starting point for the chemical mechanism to be used in multi-dimensional, multi-physics simulations of the exchange process.

The dramatic improvement in the fits to the F&M data that is made possible by the poisoning hypothesis is difficult to ignore. However, as noted previously, this explanation is bound to be controversial, primarily because it implies that the exchanges are not complete. On the other hand, the existence of poisons at the levels used in the simulations seems entirely possible. While the authors have been assured by G.W. Foltz that much care was taken in collecting the effluent data and in cleaning the Pd bed between runs, investigations into the gases used in the experiments suggest that the 5 ppm impurity in H_2 was largely H_2O and CO, both potential poisons. Moreover, even though the 100 ppm impurity in D_2 was largely H_2, it is not difficult to imagine that H_2O and/or CO were again present at the 5 ppm level. TPLUG simulations using this value have been shown to give excellent results. In truth, however, the actual level of contamination is probably not important for the simulations, because the kinetic parameters can simply adjust themselves to compensate for any change. Clearly, independent information about the strength of adsorption of various surface poisons on Pd should be incorporated into the model.

The TPLUG model is considerably less successful in reproducing the effects of deliberate CO contamination as reflected in the O&F data. Its principal failing is that it overestimates the suppression of HD formation, and in this respect it is inferior to the O&F model. However, the latter does not account well for the long-time behavior (especially at 10 ppm CO, where the data are reminiscent of the clean H→D exchange), while the TPLUG model captures it fairly well. In any case, it should also be reiterated that the kinetic parameters obtained from the TPLUG fits to the O&F data differ considerably from those extracted from the F&M data. This is due partly to differences in the data sets themselves, but a more significant issue is that reliable values for all of the kinetic parameters individually cannot be determined from the data available. In other words, combinations of parameters that are seemingly quite different can lead to comparable overall fits, so a focus on individual values is not meaningful.

Finally, while the TPLUG model can give a crude fit to the results of a highly nonisobaric and nonisothermal blowdown experiment, it cannot account for details such as the asymmetric shape and depressed maximum of the HD curve, even with the wealth of adjustable parameters in the reaction mechanism. At least for this experiment, it seems clear that the barrier to a successful simulation is not a lack of flexibility in the chemistry, but rather the inability to replicate some complex transport processes. In fact, the small (and possibly multimodal) size of the particles

involved makes it possible that the key processes are entirely different from those of the F&M and O&F experiments. This argues once again for the need to develop a multi-dimensional, multi-physics modeling capability, in conjunction with data from carefully planned and executed experiments at various temperatures.

References

1. Mitacek, P. and J.G. Aston, *Thermodynamic properties of pure palladium and its alloys with hydrogen between 30 and 300 degrees K.* Journal of the American Chemical Society, 1963. **85**(2): p. 137–141.
2. Völkl, J. and G. Alefeld, *Diffusion of hydrogen in metals*, in *Diffusion in Solids, Recent Developments*, A.S. Nowick and J.J. Burton, editors, 1975, Academic Press: New York, NY. p. 231-302.
3. Lässer, R. and K.-H. Klatt, *Solubility of hydrogen isotopes in palladium.* Physical Review B, 1983. **28**(2): p. 748–758.
4. Thomas, G.J., *SAND80-8656: Hydrogen trapping in FCC metals*, 1980, Sandia National Laboratories: Albuquerque, NM.
5. Scholten, J.J.F. and J.A. Konvalinka, *Hydrogen-deuterium equilibration and parahydrogen and orthodeuterium conversion over palladium: Kinetics and mechanism*. Journal of Catalysis, 1966. **5**(1): p. 1–17.
6. Wicke, E. and G.H. Nernst, *Phase-diagram and thermodynamics of the Pd/H_2 and Pd/D_2 system at normal temperatures: H/D separation effects.* Berichte der Bunsen-gesellschaft für physikalische Chemie, 1964. **68**(3): p. 224–235.
7. Kay, B.D., C.H.F. Peden, and D.W. Goodman, *Kinetics of hydrogen absorption by Pd(110).* Physical Review B, 1986. **34**(2): p. 817–822.
8. Lässer, R. and G.L. Powell, *Solubility of H, D, and T in Pd at low concentrations.* Physical Review B, 1986. **34**(2): p. 578–586.
9. Coluzzi, B., B. Sobha, A. Biscarini, F.M. Mazzolai, and R.A. McNicholl, *A study of diffusion of deuterium in α'-Pd deuteride by Gorsky relaxation.* Solid State Communications, 1992. **83**(8): p. 643–647.
10. Majorowski, S. and B. Baranowski, *Diffusion-coefficients of hydrogen and deuterium in highly concentrated palladium hydride and deuteride phases*. Journal of Physics and Chemistry of Solids, 1982. **43**(12): p. 1119–1127.
11. Tkacz, M. and B. Baranowski, *Solubility of hydrogen in palladium hydride at high-pressure of gaseous hydrogen.* Roczniki Chemii: Annales Societatis Chimicae Polonorum, 1976. **50**(12): p. 2159–2166.
12. Seymour, E.F.W., R.M. Cotts, and W.D. Williams, *NMR measurement of hydrogen diffusion in β-palladium hydride.* Physical Review Letters, 1975. **35**(3): p. 165–167.
13. Powell, G.L. and J.R. Kirkpatrick, *Surface conductance and the diffusion of H and D in Pd.* Physical Review B, 1991. **43**(9): p. 6968–6976.
14. Powell, G.L., J.R. Kirkpatrick, and J.W. Conant, *Surface effects in the reaction of H and D with Pd — macroscopic manifestations.* Journal of the Less-Common Metals, 1991. **172**: p. 867–872.

15. Hamilton, J., S.C. James, and W.G. Wolfer, *SAND2011-2340: Diffusional exchange of isotopes in a metal hydride sphere*, 2011, Sandia National Laboratories: Albuquerque, NM.

16. Wicke, E., *Isotope effects in palladium-hydrogen systems.* Platinum Metals Review, 1971. **15**(4): p. 144–146.

17. Sicking, G., *Isotope effects in metal hydrogen systems.* Journal of the Less Common Metals, 1984. **101**: p. 169–190.

18. Sicking, G., P. Albers, and E. Magomedbekov, *Hydrogen isotope exchange and separation in gas solid-phase systems.* Journal of the Less-Common Metals, 1983. **89**(2): p. 373–391.

19. Carstens, D.H.W. and P.D. Encinias, *Hydrogen isotope exchange over palladium metal*, 1990, Los Alamos National Laboratory: Los Alamos, NM.

20. Carstens, D.H.W. and P.D. Encinias, *Hydrogen isotopic exchange in palladium hydride.* Journal of the Less-Common Metals, 1991. **172**: p. 1331–1337.

21. Powell, G.L., *Reaction probability for exchange of hydrogen isotopes on palladium*. Physical Review B, 1992. **45**(8): p. 4505–4508.

22. Trentin, V., P.H. Brossard, and D. Schweich, *Effects of composition on the equilibrium between hydrogen isotopes and palladium.* Chemical Engineering Science, 1993. **48**(5): p. 873–879.

23. Heung, L.K. and G.C. Staack, *Hydrogen isotope exchange properties of porous solids containing hydrogen*, in 7th International Conference on Tritium Science and Technology, 2005, American Nuclear Society: La Grange Park, IL.

24. Backman, H., K. Rahkamaa-Tolonen, J. Wärnå, T. Salmi, and D.Y. Murzin, *Modelling of H_2/D_2 exchange over Pd.* Chemical Engineering Journal, 2005. **107**(1-3): p. 89–95.

25. Fukada, S., K. Fuchinoue, and M. Nishikawa, *Isotope-separation factor and isotopic exchange-rate between hydrogen and deuterium of palladium.* Journal of Nuclear Materials, 1995. **226**(3): p. 311–318.

26. Fukada, S., H. Matsuo, and N. Mitsuishi, *Application of direct numerical-analysis by Fast Fourier-Transform to isotopic exchange process in a metal hydride particle bed*. Journal of Nuclear Science and Technology, 1993. **30**(2): p. 171–180.

27. Fukada, S., T. Nakahara, and N. Mitsuishi, *Experimental and computational studies on absorption and desorption of multicomponent hydrogen isotopes from inert gas mixtures in a yttrium particle bed*. Journal of Nuclear Materials, 1990. **171**(2-3): p. 399–407.

28. Fukada, S. and M. Nishikawa, *Hydrogen isotope separation with palladium particle bed.* Fusion Engineering and Design, 1998. **39-40**: p. 995–999.

29. Charton, S., J.P. Corriou, and D. Schweich, *Modeling of hydrogen isotopes separation in a metal hydride bed.* Chemical Engineering Science, 1999. **54**: p. 103–113.

30. Foltz, G.W. and C.F. Melius, *Studies of isotopic exchange between gaseous hydrogen and palladium hydride powder*. Journal of Catalysis, 1987. **108**: p. 409–425.

31. Foltz, G.W. and C.F. Melius, *SAND86-8225: Real-time experimental measurements of isotopic exchange between gaseous hydrogen and palladium hydride powder*, 1986, Sandia National Laboratories: Albuquerque, NM.

32. Melius, C.F. and G.W. Foltz, *SAND86-8244: Modeling of temporal behavior of isotopic exchange between gaseous hydrogen and palladium hydride powder*, 1987, Sandia National Laboratories: Albuquerque, NM.

33. Outka, D.A. and G.W. Foltz, *Mechanistic studies of the isotopic-exchange reaction between gaseous hydrogen and palladium hydride powder*. Journal of Catalysis, 1991. **130**(1): p. 268–282.

34. Kee, R.J., F.M. Rupley, J.A. Miller, M.E. Coltrin, J.F. Grcar, E. Meeks, H.K. Moffat, A.E. Lutz, G. Dixon-Lewis, M.D. Smooke, J. Warnatz, G.H. Evans, R.S. Larson, R.E. Mitchell, L.R. Petzold, W.C. Reynolds, M. Caracotsios, W.E. Stewart, and P. Glarborg, *CHEMKIN Collection, Release 3.5*, 1999, Reaction Design, Inc.: San Diego, CA.

35. Griffin, J.D., T.G. Kolda, and R.M. Lewis, *SAND2006-4621: Asynchronous parallel generating set search for linearly-constrained optimization*, 2006, Sandia National Laboratories: Albuquerque, NM.

36. Caracotsios, M. and W.E. Stewart, *Sensitivity analysis of initial-value problems with mixed ODEs and algebraic equations.* Computers & Chemical Engineering, 1985. **9**(4): p. 359-365.

37. Santandrea, R. and R. Behrens, *A review of the thermodynamics and phase relationships in the palladium-hydrogen, palladium-deuterium and palladium-tritium systems*. High Temperature Materials and Processes, 1986. **7**: p. 149-169.

Appendix A. Derivation of Dissolution Equilibrium Constants

The most useful literature reference for the dissolution of H_2 and D_2 in Pd appears to be Santandrea and Behrens [37], as quoted by Charton [29]. There the equilibrium relations for reactions (R7) and (R8) are given in the form

$$\ln P_{\mathrm{H}_2} = 12.9 + 2\ln\frac{x_{\mathrm{H}}}{1-x_{\mathrm{H}}} - \frac{12070 - 10830x_{\mathrm{H}}}{T} \tag{A.1}$$

and

$$\ln P_{\mathrm{D}_2} = 12.8 + 2\ln\frac{x_{\mathrm{D}}}{1-x_{\mathrm{D}}} - \frac{11490 - 10830x_{\mathrm{D}}}{T}, \tag{A.2}$$

where P (atm) is the overpressure of the given species, T (K) is the absolute temperature, and x is the number of dissolved H or D atoms per Pd atom. These equations refer specifically to situations in which only one of the isotopes is present. To prevent future confusion about pressure units, we rewrite the equations as

$$\ln\frac{P_{\mathrm{H}_2}}{P_{\mathrm{atm}}} = 12.9 + 2\ln\frac{x_{\mathrm{H}}}{1-x_{\mathrm{H}}} - \frac{12070 - 10830x_{\mathrm{H}}}{T} \tag{A.3}$$

and

$$\ln\frac{P_{\mathrm{D}_2}}{P_{\mathrm{atm}}} = 12.8 + 2\ln\frac{x_{\mathrm{D}}}{1-x_{\mathrm{D}}} - \frac{11490 - 10830x_{\mathrm{D}}}{T}. \tag{A.4}$$

The mass-action expression for the equilibrium constant K_7, in the concentration units used by Chemkin, is

$$K_7 = \frac{[\mathrm{H_b}]^2}{[\mathrm{H_2}][\mathrm{V_b}]^2}. \tag{A.5}$$

If Γ_2 is the density of absorption sites in the bulk phase, and if one H atom can be dissolved per Pd atom, then $[\mathrm{H_b}] = \Gamma_2 x_{\mathrm{H}}$ and $[\mathrm{V_b}] = \Gamma_2(1 - x_{\mathrm{H}})$. Furthermore, from the ideal gas law, $[\mathrm{H_2}] = P_{\mathrm{H}_2}/RT$; therefore

$$K_7 = \frac{RT}{P_{\mathrm{H}_2}}\left(\frac{x_{\mathrm{H}}}{1-x_{\mathrm{H}}}\right)^2. \tag{A.6}$$

Rearrangement gives

$$\ln P_{H_2} = \ln \frac{RT}{K_7} + 2\ln \frac{x_H}{1 - x_H}, \tag{A.7}$$

which is clearly similar to (A.3). Eliminating P_{H_2} and solving for the equilibrium constant gives

$$K_7 = 2.498 \times 10^{-6} \frac{RT}{P_{atm}} \exp\left(\frac{12070 - 10830 x_H}{T}\right). \tag{A.8}$$

Finally, we substitute for R and P_{atm} in cgs units and multiply top and bottom in the exponential by R in kJ/mol to obtain

$$K_7 = 2.050 \times 10^{-4} T \exp\left(\frac{100.35 - 90.04 x_H}{RT}\right), \tag{A.9}$$

which is the same as (12). The derivation of (13) is completely analogous.

Clearly, both (12) and (13) imply a coverage-dependent heat of reaction, which is a form of nonideal behavior. Because of this, the expressions must be generalized for the case in which both isotopes are present. An obvious solution is to use the sum $x_H + x_D$ in both equations:

$$K_7 = 2.050 \times 10^{-4} T \exp\left[\frac{100.35 - 90.04\left(x_H + x_D\right)}{RT}\right] \tag{A.10}$$

$$K_8 = 2.265 \times 10^{-4} T \exp\left[\frac{95.53 - 90.04\left(x_H + x_D\right)}{RT}\right] \tag{A.11}$$

However, this is not the most general solution, because there is no fundamental requirement that the coefficients of x_H and x_D in a given equation be equal. On the other hand, it will be shown in Appendix B that the new cross-coefficients in the two equations must in fact be equal, and this leads to (14) and (15) as the final equilibrium expressions.

Appendix B. Calculation of Thermodynamic Properties for Non-Isothermal Simulations

To solve the energy balance in (for example) a Chemkin-based application, thermodynamic data coefficients are required for each species. Often these are not known for at least some of the surface and bulk species, but they can be extracted from equilibrium constants for reactions in which the species are involved, as will now be shown.

Considering first (R1), the rate constant in the forward direction is expressed in the generalized Arrhenius form

$$k_1 = A_1 T^{n_1} \exp\left(-\frac{E_1}{RT}\right), \tag{B.1}$$

with an analogous expression for the reverse direction. The equilibrium constant for the reaction is the ratio of rate constants:

$$K_1 = \frac{A_1}{A_{-1}} T^{n_1 - n_{-1}} \exp\left(-\frac{E_1 - E_{-1}}{RT}\right). \tag{B.2}$$

Note that this equilibrium constant is in *concentration* units, because the rate constants used by Chemkin are in those units. The equilibrium constant in terms of partial pressures ($\hat{K}_i$) can be written in terms of the standard free energy of reaction, because the thermodynamic properties for gas-phase species use a standard state expressed in terms of pressure:

$$\hat{K}_1 = \exp\left(-\frac{\Delta G_1^0}{RT}\right). \tag{B.3}$$

The two equilibrium constants can also be written in terms of pressure/concentration ratios as

$$K_1 = \frac{\left[\mathrm{H_s}\right]^2}{\left(P_{\mathrm{H_2}}/RT\right)\left[\mathrm{V_s}\right]^2} \tag{B.4}$$

and

$$\hat{K}_1 = \frac{\left[\mathrm{H_s}\right]^2}{\left(P_{\mathrm{H_2}}/P_{\mathrm{atm}}\right)\left[\mathrm{V_s}\right]^2}, \tag{B.5}$$

respectively, assuming that the standard-state pressure is 1 atm. (Note that, in accordance with (B.2) and (B.3), $\hat{K}_1$ is dimensionless while K_1 is not.) Thus

$$K_1 = \hat{K}_1 \frac{RT}{P_{\mathrm{atm}}}. \tag{B.6}$$

Substituting from (B.2) and (B.3),

$$\Delta G_1^0 = E_1 - E_{-1} - RT \ln\left(\frac{A_1 P_{\mathrm{atm}}}{A_{-1} R} T^{n_1 - n_{-1} - 1}\right). \tag{B.7}$$

Of course, ΔG_1^0 can also be written as

$$\Delta G_1^0 = 2G_{\mathrm{H_s}}^0 - G_{\mathrm{H_2}}^0 - 2G_{\mathrm{V_s}}^0, \tag{B.8}$$

so

$$2\left(G^0_{\mathrm{H_s}} - G^0_{\mathrm{V_s}}\right) = E_1 - E_{-1} - RT\ln\left(\frac{A_1 P_{\mathrm{atm}}}{A_{-1}R}\right) - \left(n_1 - n_{-1} - 1\right)RT\ln T + G^0_{\mathrm{H_2}}. \tag{B.9}$$

This gives the difference in standard-state free energies of H_s and V_s entirely in terms of known quantities. Note that it does not give the free energies individually; however, because V_s is irreducible, it plays the role of a chemical element, and its thermodynamic properties can therefore be assigned arbitrarily (at a given temperature).

Use of the Gibbs-Helmholtz equation

$$\frac{\partial\left(G_i^0/T\right)}{\partial T} = -\frac{H_i^0}{T^2} \tag{B.10}$$

yields

$$\frac{H^0_{\mathrm{H_s}}}{RT} - \frac{H^0_{\mathrm{V_s}}}{RT} = \frac{1}{2}\left(\frac{H^0_{\mathrm{H_2}}}{RT} + \frac{E_1 - E_{-1}}{RT} + n_1 - n_{-1} - 1\right). \tag{B.11}$$

Similarly, use of

$$\frac{\partial G_i^0}{\partial T} = -S_i^0 \tag{B.12}$$

gives

$$\frac{S^0_{\mathrm{H_s}}}{R} - \frac{S^0_{\mathrm{V_s}}}{R} = \frac{1}{2}\left[\frac{S^0_{\mathrm{H_2}}}{R} + \left(n_1 - n_{-1} - 1\right)\ln T + n_1 - n_{-1} - 1 + \ln\left(\frac{A_1 P_{\mathrm{atm}}}{A_{-1}R}\right)\right]. \tag{B.13}$$

The polynomial expansions used in the Chemkin database are

$$\frac{H_i^0}{RT} = a_{1i} + \frac{a_{2i}}{2}T + \frac{a_{3i}}{3}T^2 + \frac{a_{4i}}{4}T^3 + \frac{a_{5i}}{5}T^4 + \frac{a_{6i}}{T} \tag{B.14}$$

and

$$\frac{S_i^0}{R} = a_{1i}\ln T + a_{2i}T + \frac{a_{3i}}{2}T^2 + \frac{a_{4i}}{3}T^3 + \frac{a_{5i}}{4}T^4 + a_{7i}. \tag{B.15}$$

Substituting (B.14) into (B.11) and matching coefficients yields

$$a_{1,\mathrm{H_s}} - a_{1,\mathrm{V_s}} = \frac{1}{2}\left(a_{1,\mathrm{H_2}} + n_1 - n_{-1} - 1\right) \tag{B.16}$$

$$a_{j,\mathrm{H_s}} - a_{j,\mathrm{V_s}} = \frac{1}{2}a_{j,\mathrm{H_2}} \quad \text{for} \quad j = 2,\ldots,5 \tag{B.17}$$

$$a_{6,\mathrm{H_s}} - a_{6,\mathrm{V_s}} = \frac{1}{2}\left(a_{6,\mathrm{H_2}} + \frac{E_1 - E_{-1}}{R}\right). \tag{B.18}$$

Likewise, substitution of (B.15) into (B.13) gives (B.16) and (B.17) as well as

$$a_{7,\mathrm{H_s}} - a_{7,\mathrm{V_s}} = \frac{1}{2}\left[a_{7,\mathrm{H_2}} + n_1 - n_{-1} - 1 + \ln\left(\frac{A_1 P_{\mathrm{atm}}}{A_{-1}R}\right)\right]. \tag{B.19}$$

Reaction (R3) is handled in the same way and provides the thermodynamic coefficients for D_s.

Now consider reaction (R5). In this case, because no gas-phase species are involved and because sites are conserved, even the concentration equilibrium constant is dimensionless. On the other hand, the coverage dependence of the reverse activation energy is a complicating factor, because it implies nonideal thermodynamic behavior. The polynomial coefficients in the thermodynamic data can only be used to compute standard-state thermodynamic properties as functions of temperature. Therefore, it is necessary to determine how the coverage parameters can be accounted for properly in computing thermodynamic properties under actual conditions.

In Chemkin, coverage dependence of a rate constant does *not* affect the computation of the equilibrium constant. In other words, mass-action kinetics can be overridden, but nonideal thermodynamic behavior is not accounted for. The latter can be overcome by specifying both forward and reverse rate constants rather than asking Chemkin to compute the equilibrium constant internally. However, it leaves open the question of what to use in compiling the thermodynamic polynomial coefficients for H_b.

Because the coverage dependence arises from actual data on the dissolution of hydrogen in Pd, it is simplest to return to reaction (R7) in evaluating the thermodynamic properties of H_b. The equilibrium constant for this reaction is given by (A.10) (or a slight generalization of this). However, it is important to note that this concentration equilibrium constant is in fact not a constant at all, because of the dependence on site fractions. In a rigorous thermodynamic analysis, the true equilibrium constant must be written in terms of activities rather than concentrations (or site fractions, since the site density cancels). The site fraction and the activity are often treated as identical, but that is not true for a nonideal system.

Assuming that the gas phase is ideal, the true equilibrium constant is

$$\hat{K}_7 = \frac{\left(x_{\mathrm{H}}\gamma_{\mathrm{H}}\right)^2}{\left(P_{\mathrm{H_2}}/P_{\mathrm{atm}}\right)\left[\left(1 - x_{\mathrm{H}} - x_{\mathrm{D}}\right)\gamma_{\mathrm{V}}\right]^2}, \tag{B.20}$$

where the γ_i are (dimensionless) activity coefficients. K_7 can be expressed in analogous form as

$$K_7 = \frac{x_{\mathrm{H}}^2}{\left(P_{\mathrm{H}_2}/RT\right)\left(1 - x_{\mathrm{H}} - x_{\mathrm{D}}\right)^2}. \tag{B.21}$$

Therefore

$$\hat{K}_7 = K_7 \frac{P_{\mathrm{atm}}}{RT}\left(\frac{\gamma_{\mathrm{H}}}{\gamma_{\mathrm{V}}}\right)^2, \tag{B.22}$$

which, when combined with (A.10), yields

$$\hat{K}_7 = 2.498 \times 10^{-6} \exp\left[\frac{100.35 - 90.04\left(x_{\mathrm{H}} + x_{\mathrm{D}}\right)}{RT}\right]\left(\frac{\gamma_{\mathrm{H}}}{\gamma_{\mathrm{V}}}\right)^2. \tag{B.23}$$

The same analysis for reaction (R8) gives

$$\hat{K}_8 = 2.760 \times 10^{-6} \exp\left[\frac{95.53 - 90.04\left(x_{\mathrm{H}} + x_{\mathrm{D}}\right)}{RT}\right]\left(\frac{\gamma_{\mathrm{D}}}{\gamma_{\mathrm{V}}}\right)^2. \tag{B.24}$$

Because the left-hand sides of (B.23) and (B.24) are functions only of temperature, the same must be true of the right-hand sides. Therefore,

$$\frac{\gamma_{\mathrm{H}}}{\gamma_{\mathrm{V}}} = f(T) \exp\left[\frac{45.02\left(x_{\mathrm{H}} + x_{\mathrm{D}}\right)}{RT}\right] \tag{B.25}$$

and

$$\frac{\gamma_{\mathrm{D}}}{\gamma_{\mathrm{V}}} = g(T) \exp\left[\frac{45.02\left(x_{\mathrm{H}} + x_{\mathrm{D}}\right)}{RT}\right], \tag{B.26}$$

where $f(T)$ and $g(T)$ are unknown functions.

The third relation needed to determine the three activity coefficients is provided by the Gibbs-Duhem equation. For variations at constant temperature and pressure, this takes the form

$$\sum_k x_k d\ln\gamma_k = 0, \tag{B.27}$$

or, in this case,

$$x_{\mathrm{H}} d\ln\gamma_{\mathrm{H}} + x_{\mathrm{D}} d\ln\gamma_{\mathrm{D}} + x_{\mathrm{V}} d\ln\gamma_{\mathrm{V}} = 0. \tag{B.28}$$

From (B.25) and (B.26),

$$d\ln\gamma_{\mathrm{H}} = d\ln\gamma_{\mathrm{D}} = d\ln\gamma_{\mathrm{V}} - \frac{45.02}{RT}dx_{\mathrm{V}}, \tag{B.29}$$

and substitution into (B.28) yields

$$d\ln\gamma_{\mathrm{V}} = \frac{45.02}{RT}\left(1 - x_{\mathrm{V}}\right)dx_{\mathrm{V}}. \tag{B.30}$$

This is integrated subject to the condition that $\gamma_{\mathrm{V}} \to 1$ as $x_{\mathrm{V}} \to 1$, implying that the standard state for the "solvent" vacancies is a system with no hydrogen present:

$$\gamma_{\mathrm{V}} = \exp\left[\frac{-22.51}{RT}\left(1 - x_{\mathrm{V}}\right)^2\right] = \exp\left[\frac{-22.51}{RT}\left(x_{\mathrm{H}} + x_{\mathrm{D}}\right)^2\right]. \tag{B.31}$$

Substituting this into (B.25) and (B.26) gives

$$\gamma_{\mathrm{H}} = f(T)\exp\left[\frac{22.51}{RT}\left(1 - x_{\mathrm{V}}^2\right)\right] \tag{B.32}$$

and

$$\gamma_{\mathrm{D}} = g(T)\exp\left[\frac{22.51}{RT}\left(1 - x_{\mathrm{V}}^2\right)\right], \tag{B.33}$$

respectively. Because the site fractions x_{H} and x_{D} can, in principle, vary all the way from 0 to 1, it is permissible (and convenient) to adopt the symmetric or Raoult's law convention for the activity coefficients, namely that $\gamma_k \to 1$ as $x_k \to 1$ for every species. It follows that

$$f(T) = g(T) = \exp\left(-\frac{22.51}{RT}\right) \tag{B.34}$$

and therefore

$$\gamma_{\mathrm{H}} = \gamma_{\mathrm{D}} = \exp\left(-\frac{22.51}{RT}x_{\mathrm{V}}^2\right). \tag{B.35}$$

Because the effects of x_{H} and x_{D} on the enthalpy of dissolution are treated as identical, it is not surprising that γ_{H} and γ_{D} are also identical. In fact, (B.31) and (B.35) together show that $\mathrm{H_b}$ and $\mathrm{D_b}$ behave as a single species, at least as far as the nonideality is concerned. Consistent with this, note that $\gamma_{\mathrm{H}} \to 1$ as $x_{\mathrm{H}} \to 1$ *or* $x_{\mathrm{D}} \to 1$.

Now, substitution of (B.35) and (B.31) into (B.23) gives

$$\hat{K}_7 = 2.498 \times 10^{-6} \exp\left(\frac{55.33}{RT}\right), \tag{B.36}$$

confirming that $\hat{K}_7$, the true equilibrium constant, is a function only of temperature, as noted above. The corresponding result for $\hat{K}_8$ is

$$\hat{K}_8 = 2.760 \times 10^{-6} \exp\left(\frac{50.51}{RT}\right). \tag{B.37}$$

These equations can be used to extract the polynomial coefficients for H_b and D_b in their standard states by applying equations analogous to (B.3) and (B.8). However, the results will not be useful by themselves, because the thermodynamic properties in an actual system will be strongly influenced by nonidealities, and these must somehow be taken into account. Chemkin, in particular, is not currently configured to do this, so it must be handled in the reactor simulation code.

To see what is involved, note that the partial molar Gibbs free energy (i.e., the chemical potential) of a given species is, in general,

$$G_i = G_i^0 + RT \ln x_i \gamma_i \, . \tag{B.38}$$

Application of the Gibbs-Helmholtz equation gives

$$H_i = -T^2 \frac{\partial (G_i / T)}{\partial T} = H_i^0 - RT^2 \frac{\partial \ln \gamma_i}{\partial T}. \tag{B.39}$$

This shows how the standard state enthalpy obtained (for example) from a Chemkin call must be corrected for nonidealities. For the specific case of H_b, substitution from (B.35) yields

$$H_{\mathrm{H_b}} = H_{\mathrm{H_b}}^0 - 22.51 x_{\mathrm{V}}^2, \tag{B.40}$$

where the numerical constant has units of kJ/mol. The result for D_b is analogous, while that for V_b is

$$H_{\mathrm{V_b}} = H_{\mathrm{V_b}}^0 - 22.51 (1 - x_{\mathrm{V}})^2 . \tag{B.41}$$

Again, these corrections must be implemented in the application code if the energy balance is to be accurate.

Presumably, corrected entropies are not needed as long as equilibrium constants from Chemkin are not used to compute reverse rate constants. However, for completeness, the relevant results are

$$S_i = -\frac{\partial G_i}{\partial T} = S_i^0 - R\left(\ln x_i + \ln \gamma_i + T\frac{\partial \ln \gamma_i}{\partial T}\right) \tag{B.42}$$

$$S_{\mathrm{H_b}} = S_{\mathrm{H_b}}^0 - R\ln x_{\mathrm{H}} \tag{B.43}$$

$$S_{\mathrm{D_b}} = S_{\mathrm{D_b}}^0 - R\ln x_{\mathrm{D}} \tag{B.44}$$

$$S_{\mathrm{V_b}} = S_{\mathrm{V_b}}^0 - R\ln x_{\mathrm{V}}. \tag{B.45}$$

These show that there are, in fact, no nonideality corrections to the entropies. In retrospect this is not surprising, because the coverage dependence of the heat of dissolution is strictly an enthalpy effect.

Finally, recall that the dependence of K_7 on x_{D} in (A.10), and of K_8 on x_{H} in (A.11), is merely an assumption. It is useful to know the extent to which this can be generalized. Therefore, suppose instead that

$$K_7 = 2.050\times 10^{-4} T \exp\left(\frac{100.35 - 90.04x_{\mathrm{H}} - 2\lambda x_{\mathrm{D}}}{RT}\right) \tag{B.46}$$

and

$$K_8 = 2.265\times 10^{-4} T \exp\left(\frac{95.53 - 2\beta x_{\mathrm{H}} - 90.04x_{\mathrm{D}}}{RT}\right), \tag{B.47}$$

where λ and β are unspecified at this point. Then (B.25) and (B.26) become

$$\frac{\gamma_{\mathrm{H}}}{\gamma_{\mathrm{V}}} = f(T)\exp\left(\frac{45.02x_{\mathrm{H}} + \lambda x_{\mathrm{D}}}{RT}\right) \tag{B.48}$$

and

$$\frac{\gamma_{\mathrm{D}}}{\gamma_{\mathrm{V}}} = g(T)\exp\left(\frac{\beta x_{\mathrm{H}} + 45.02x_{\mathrm{D}}}{RT}\right). \tag{B.49}$$

Substitution into (B.28), together with the fact that $x_{\mathrm{D}} = 1 - x_{\mathrm{V}} - x_{\mathrm{H}}$, gives

$$d\ln\gamma_{\mathrm{V}} = -\frac{1}{RT}\left\{\left[45.02\left(2x_{\mathrm{H}} - 1 + x_{\mathrm{V}}\right) - \lambda x_{\mathrm{H}} + \beta\left(1 - x_{\mathrm{V}} - x_{\mathrm{H}}\right)\right]dx_{\mathrm{H}} + \left[45.02\left(-1 + x_{\mathrm{V}} + x_{\mathrm{H}}\right) - \lambda x_{\mathrm{H}}\right]dx_{\mathrm{V}}\right\}. \tag{B.50}$$

Clearly, at constant temperature and pressure, γ_{V} can be treated as a function of only x_{H} and x_{V}. Therefore, the following partial derivatives can be formed:

$$\frac{\partial \ln \gamma_V}{\partial x_H} = -\frac{1}{RT}\left[45.02\left(2x_H - 1 + x_V\right) - \lambda x_H + \beta\left(1 - x_V - x_H\right)\right] \tag{B.51}$$

$$\frac{\partial^2 \ln \gamma_V}{\partial x_H \partial x_V} = \frac{\beta - 45.02}{RT} \tag{B.52}$$

$$\frac{\partial \ln \gamma_V}{\partial x_V} = -\frac{1}{RT}\left[45.02\left(-1 + x_V + x_H\right) - \lambda x_H\right] \tag{B.53}$$

$$\frac{\partial^2 \ln \gamma_V}{\partial x_V \partial x_H} = \frac{\lambda - 45.02}{RT}. \tag{B.54}$$

Comparison of (B.52) and (B.54) shows that λ must be equal to β, although the value of this single quantity is then arbitrary. This conclusion is intuitively reasonable, as it suggests that the enthalpy effect of absorbing both an H and a D is independent of the order in which this is done.

Of course, if the generalized expressions for K_7 and K_8 are used, then the details of the thermodynamic property calculations are altered. The analysis is fairly complex, but the resulting expressions for the activity coefficients are

$$RT \ln \gamma_V = -22.51\left(1 - x_V\right)^2 + \left(45.02 - \beta\right) x_H x_D, \tag{B.55}$$

$$RT \ln \gamma_H = -22.51 x_V^2 - \left(45.02 - \beta\right) x_D \left(1 - x_H\right), \tag{B.56}$$

and

$$RT \ln \gamma_D = -22.51 x_V^2 - \left(45.02 - \beta\right) x_H \left(1 - x_D\right). \tag{B.57}$$

The new enthalpy corrections follow immediately from these, while (B.36) and (B.37) are unaltered.

Appendix C. Parameter Decoupling During Optimization

In the effort to find the best fit to a set of time-dependent isotope exchange data, the first two adjustable parameters are the site densities for the two solid phases (surface and bulk). While a reasonable estimate for the latter could be made in advance, its treatment in Chemkin as a *surface* density could make this problematic. In any case, the remaining adjustable parameters (except β) are those associated with the kinetics of the reactions — specifically, those single-direction reactions that are not subject to thermodynamic constraints. It would be presumptuous to treat the temperature exponents (such as n_1 in (B.1)) as adjustable, given the inevitable noise in the data, so these are set to zero. Thus, there are just two free parameters per reaction. The most obvious course of action is to adjust both the pre-exponential factor (e.g., A_1) and the activation energy (e.g., E_1). (Of course, the latter is not relevant for purely isothermal simulations, so this discussion is for the general case.) However, the tight coupling between these parameters would lead to an inefficient optimization process. There is also a tight coupling

between the pre-exponential factor and the site density, and this would likewise cause problems. We now explain this in more detail and show how the efficiency can be improved.

Consider the reaction

$$\mathrm{B} + \mathrm{D} \rightarrow \text{products}, \tag{C.1}$$

where B and D are surface species. The mass action expression for the reaction rate is simply

$$\dot{s} = k c_{\mathrm{B}} c_{\mathrm{D}}, \tag{C.2}$$

where the c_i (mol/cm^2) are surface concentrations. Assuming a simple Arrhenius form for k (cm^2/mol·s), this can be rewritten as

$$\dot{s} = A \exp\left(-\frac{E}{RT}\right) \Gamma^2 x_{\mathrm{B}} x_{\mathrm{D}} , \tag{C.3}$$

where Γ (mol/cm^2) is the site density and the x_i are site fractions. Parameters A (cm^2/mol·s), E (kJ/mol), and Γ are assumed to be unknown and are to be varied to optimize the fit to the data. They could be varied independently, but this has two drawbacks:

(1) Varying E changes not only the temperature dependence of the rate constant, but also its magnitude at any temperature. This causes A and E to be strongly coupled, in the sense that any change in E is likely to require an offsetting change in A.

(2) In varying Γ, one would like to change only the phase capacity, but (C.3) shows that the reaction rate would be changed as well. It is desirable to insulate $\dot{s}$ from changes in Γ, which is equivalent to decoupling Γ and A.

To address the first issue, we first define a reference temperature T_r. The rate constant at this temperature is obviously

$$k_r = A \exp\left(-\frac{E}{RT_r}\right), \tag{C.4}$$

and thus

$$\dot{s} = k_r \exp\left[-\frac{E}{R}\left(\frac{1}{T} - \frac{1}{T_r}\right)\right] \Gamma^2 x_{\mathrm{B}} x_{\mathrm{D}}. \tag{C.5}$$

With this formulation, a variation in E alone has little effect on the reaction rate near T_r, so the desired decoupling is achieved.

To deal with the second issue, it is necessary to make k_r a function of Γ — specifically, proportional to Γ^{-2}. Thus, we define a reference site density Γ_r and let k_{rr} be the value of k_r associated with it, i.e.,

$$k_r = k_{rr}\left(\frac{\Gamma_r}{\Gamma}\right)^2. \tag{C.6}$$

Substituting into (C.5),

$$\dot{s} = k_{rr}\Gamma_r^2 \exp\left[-\frac{E}{R}\left(\frac{1}{T}-\frac{1}{T_r}\right)\right]x_{\mathrm{B}}x_{\mathrm{D}}. \tag{C.7}$$

This shows that, if the surface composition in terms of site fractions is fixed, then Γ has no effect on the reaction rate. The three adjustable parameters should therefore be k_{rr}, E, and Γ (the latter of which, as noted above, is still needed to represent the phase capacity in the conservation equations). Note, however, that the rate constant provided to Chemkin must be the one that multiplies the surface concentrations, not the site fractions. To obtain this, we simply divide (C.7) by $\Gamma^2 x_{\mathrm{B}} x_{\mathrm{D}}$, as dictated by (C.3). Thus, the expression that must be represented in the Chemkin input file is

$$k = k_{rr}\left(\frac{\Gamma_r}{\Gamma}\right)^2 \exp\left[-\frac{E}{R}\left(\frac{1}{T}-\frac{1}{T_r}\right)\right]. \tag{C.8}$$

Obviously, analogous formulas apply for other reaction orders, with only the surface species being relevant in this regard.

Appendix D. Assessment of Foltz & Melius Chemistry

Instead of the more general reaction set consisting of (R1)–(R3), (R5), and (R6), Foltz and Melius [30] used a simple two-step mechanism consisting of the following reactions:

$$\mathrm{D_2 + H_b \Leftrightarrow HD + D_b} \tag{R10}$$

$$\mathrm{HD + H_b \Leftrightarrow H_2 + D_b} \tag{R11}$$

(They actually wrote these in terms of surface rather than bulk atoms, but they did not distinguish between the two.) They then assumed the following relationships to hold:

$$\frac{k_{11}}{k_{10}} = \frac{1}{2} \tag{D.1}$$

$$\frac{k_{10}}{k_{-10}} = \frac{2}{\alpha} \tag{D.2}$$

$$\frac{k_{11}}{k_{-11}} = \frac{1}{2\alpha}, \tag{D.3}$$

where α is referred to as the isotope separation factor. It is of interest to assess the accuracy of these relationships. The first step is to note that subtracting (R11) from (R10) yields (R9); therefore, the equilibrium constants for the three reactions are related by

$$K_9 = K_{10}K_{11}^{-1}. \tag{D.4}$$

It follows immediately that

$$\frac{k_{10}k_{-11}}{k_{-10}k_{11}} = K_9, \tag{D.5}$$

which provides one constraint on the set of four rate constants. To obtain another, consider the pair of dissolution reactions (R7) and (R8). Subtracting the former from the latter gives the overall exchange reaction

$$\mathrm{D_2 + 2H_b \Leftrightarrow H_2 + 2D_b}. \tag{R12}$$

However, this is also the result of adding (R10) and (R11). It follows that

$$K_8K_7^{-1} = K_{10}K_{11}, \tag{D.6}$$

and therefore

$$\frac{k_{10}k_{11}}{k_{-10}k_{-11}} = \frac{K_8}{K_7}. \tag{D.7}$$

Together, (D.5) and (D.7) give

$$\frac{k_{10}}{k_{-10}} = \left(\frac{K_8K_9}{K_7}\right)^{1/2} \tag{D.8}$$

and

$$\frac{k_{11}}{k_{-11}} = \left(\frac{K_8}{K_7K_9}\right)^{1/2}. \tag{D.9}$$

These would appear to be the only constraints that can be imposed purely on the basis of thermodynamics. They are to be compared with the corresponding F&M relationships (D.2) and (D.3).

Recall that K_9 is given by (11), while reasonably accurate expressions for K_7 and K_8 are (A.10) and (A.11), respectively. (The slightly more general results (14) and (15) are not useful here, because β is unknown.) Substituting into (D.8) and (D.9) gives

$$\frac{k_{10}}{k_{-10}} = 2.165 \exp\left(-\frac{2.73}{RT}\right) \tag{D.10}$$

and

$$\frac{k_{11}}{k_{-11}} = 0.510 \exp\left(-\frac{2.09}{RT}\right). \tag{D.11}$$

Evaluating at 299 K, the temperature used by F&M,

$$\frac{k_{10}}{k_{-10}} = 0.722 \tag{D.12}$$

and

$$\frac{k_{11}}{k_{-11}} = 0.220. \tag{D.13}$$

The corresponding relationships from (D.2) and (D.3), using the F&M value of $\alpha = 2.4$, are

$$\frac{k_{10}}{k_{-10}} = 0.833 \tag{D.14}$$

and

$$\frac{k_{11}}{k_{-11}} = 0.208. \tag{D.15}$$

These are not greatly in error. Perfect agreement could not have been expected, because F&M implicitly assumed a constant value of $K_9 = 4$ in using (D.1)−(D.3). Looked at differently, use of the same α in both (D.2) and (D.3) overconstrains the problem and results in a thermodynamic inconsistency. To clarify this, suppose that (D.3) is replaced by

$$\frac{k_{11}}{k_{-11}} = \frac{1}{2\hat{\alpha}}. \tag{D.16}$$

Comparison of (D.2) with (D.12) and (D.16) with (D.13) gives $\alpha = 2.77$ and $\hat{\alpha} = 2.27$. The fact that these are different confirms that (D.1)−(D.3) are not completely consistent, although it is reassuring that the value of $\alpha = 2.4$ used by F&M is close to the average of the two values computed here.

Note further that the generalization of (D.3) as (D.16) is not the only option for eliminating the inconsistency. The factors of 2 that appear in (D.2) and (D.3) (as well as (D.1)) are derived from statistical considerations and ultimately give rise to the erroneous value of 4 for K_9. Therefore, a potentially appealing alternative is to retain a single value for α but to modify (D.2) and (D.3) as follows:

$$\frac{k_{10}}{k_{-10}} = \frac{\phi}{\alpha} \tag{D.17}$$

$$\frac{k_{11}}{k_{-11}} = \frac{1}{\phi\alpha}. \tag{D.18}$$

Comparing with (D.12) and (D.13), respectively, yields α = 2.51 and ϕ = 1.81. Thus, in this manner, thermodynamic consistency can be achieved while retaining the symmetry of the F&M relationships.